

Rapid computer-aided automatic segmentation of enhanced tissue in
late gadolinium enhancement cardiovascular magnetic resonance
clinical examinations for providing improved healthcare management and
diagnostics for long-standing persistent atrial fibrillation patients

Archontis Giannakidis^{1,2,†}, Eva Nyktari¹, Jennifer Keegan^{1,2},
Iain Pierce^{1,2}, Irina Suman Horduna¹, Shouvik Haldar¹,
Dudley J. Pennell^{1,2}, Raad Mohiaddin¹, Tom Wong¹, David N. Firmin^{1,2}

1. Cardiovascular Biomedical Research Unit, Royal Brompton Hospital, London, UK
2. National Heart & Lung Institute, Imperial College London, London, UK

† Corresponding author: A.Giannakidis@rbht.nhs.uk

May 2015

Abstract

Atrial fibrillation (AF) is the most common heart rhythm disorder. In order for late Gd enhancement cardiovascular magnetic resonance (LGE CMR) to ameliorate the AF management, the ready availability of the accurate enhancement segmentation is required. However, the computer-aided segmentation of enhancement in LGE CMR of AF is still an open question. Additionally, the number of centres that have reported successful application of LGE CMR to guide clinical AF strategies remains low, while the debate on LGE CMR's diagnostic ability for AF still holds. The aim of this study is to propose a method that reliably distinguishes enhanced (abnormal) from non-enhanced (healthy) tissue within the left atrial wall of (pre-ablation and three months post-ablation) LGE CMR data-sets from long-standing persistent AF patients studied at our centre.

Enhancement segmentation was achieved by employing thresholds benchmarked against the statistics of the whole left atrial blood-pool (LABP). The test-set cross-validation mechanism was applied to determine the input feature representation and algorithm that best predict enhancement threshold levels.

Global normalized intensity threshold levels $T_{PRE}=1 \frac{1}{4}$ and $T_{POST}=1 \frac{5}{8}$ were found to segment enhancement in data-sets acquired pre-ablation and at three months post-ablation, respectively. The segmentation results were corroborated by using visual inspection of LGE CMR brightness levels and one endocardial bipolar voltage map. The measured extent of pre-ablation fibrosis fell within the normal range for the specific arrhythmia phenotype. 3D volume renderings of segmented post-ablation enhancement emulated the expected ablation lesion patterns. By comparing our technique with other related approaches that proposed different threshold levels (although they also relied on reference regions from within the LABP) for segmenting enhancement in LGE CMR data-sets of AF patients, we illustrated that the cut-off levels employed by other centres may not be usable for clinical studies performed in our centre.

The proposed technique has great potential for successful employment in the AF management within our centre. It provides a highly desirable validation of the LGE CMR technique for AF studies. Inter-centre differences in the CMR acquisition protocol and image analysis strategy inevitably impede the selection of a universally optimal algorithm for segmentation of enhancement in AF studies.

Keywords

late gadolinium enhancement, cardiovascular magnetic resonance, atrial fibrillation, segmentation, fibrosis, ablation lesion, three-dimensional visualization, left atrium, electro-anatomical mapping

1. Introduction

1.1 Clinical backdrop

Atrial fibrillation (AF) occurs when chaotic electrical activity develops in the atrial walls, causing the atrial muscle cells to contract irregularly and rapidly. Apart from electrical and contractile remodelling, it is well established [1,2] that AF is also associated with structural remodelling, including left atrial fibrosis. Fibrotic changes in the left atrial substrate have been postulated [1,2] to underlie the persistence and sustainability of AF. AF is the most common heart rhythm disorder; it affects 2% of the population, a figure that is rising fast [3]. AF has been connected [4,5,6] with a notable reduction in quality of life, poor mental health, disability, and a significant increase in the risk of stroke, dementia, and death. It is a serious and growing drain on the purse of healthcare providers worldwide, with the estimated [3] annual (2005) cost of AF treatment in USA to be \$6.65 billion.

Ablation (by catheter or surgical techniques) of the left atrium (LA) has been widely accepted [7] as a clinical therapy for AF patients that are refractory to anti-arrhythmic medicines and direct current cardio-version. It is based on the principle of restoring sinus rhythm by forming lesions (scar tissue) that either electrically isolate the triggers of ectopic beats or modify the AF-favouring left atrial substrate. Despite efforts to improve targeting and delivery of AF ablation, the long-term durable restoration of sinus rhythm is achieved only for a moderate part of the AF population with AF-free rates after a single ablation to vary [8,9] between 30-50% at five years follow-up. Patients who fail the initial ablation commonly undergo redo procedures, thus reducing the cost-effectiveness of AF ablation and increasing the risk of associated complications.

The high failure rate of ablation in AF patients is in part attributable to: (i) Difficulty in identifying befitting ablation candidates. Excluding patients unlikely to benefit from AF ablation would improve the success rates. (ii) Incapability to establish the ideal ablation strategy for every patient. Experts have agreed [10] that one ablation strategy does not fit all AF patients. (iii) Limited information about the location and extent of the ablation-induced injury during and/or after the procedure. Such information could be used to identify gaps in ablation lines and guide initial/redo operations. (iv) Restricted knowledge of the lesion set permanence at the procedure time. This renders the ablation end-point definition extremely dubious. Silent electrograms in the ablated area are frequently temporary. Indeed, restored electrical connection at previously targeted sites almost invariably takes place in patients who return for a repeat procedure [10,11].

The advent of late gadolinium (Gd) enhancement cardiovascular magnetic resonance (LGE CMR) more than a decade ago allowed the differentiation between normal and diseased left ventricular myocardium [12]. Its foundation lies in the slow washout kinetics of Gd agents in abnormal tissue. In brief, the delayed removal of Gd from abnormal cardiac tissue areas results in them being detectable as enhanced (i.e., brighter than healthy myocardium) zones. More recently, three-dimensional (3D) high spatial resolution LGE CMR has shown promise in increasing the success

rates of AF ablation procedure. It offers the potential to deal with the AF ablation failing causes described above by non-invasively imaging left atrial (i) gradual native fibrosis associated with AF [13-30], (ii) iatrogenic ablation-induced lesion sets [11,15,16,18,22,26,27,31-47]. The former LGE CMR-derived tissue characterization has been suggested to (i) assess patient suitability for AF ablation by identifying potential non-responders [13-16,18,19,23], (ii) define the most appropriate ablation approach [15,16,21], (iii) select anticoagulation strategy [16-18]. Correspondingly, the latter LGE CMR-derived tissue visualization has been proposed to (i) guide redo ablation procedures [16,18,22,32,36,47], (ii) deter the inadequate/ample lesion formation in the real-time (i.e., time-of-procedure) setting by assisting in the definition of a punctual ablation endpoint [16,38-40,42-44]. The use of LGE CMR to define native left atrial fibrosis associated with AF has been corroborated by histopathology studies [23,48]. Similarly, a comprehensive histological validation of using LGE CMR to characterize AF ablation-induced wall injury has been presented [49].

1.2 Challenges & current situation in the enhancement segmentation literature

The potential role of LGE CMR in the AF management discussed in the previous section underlines the great necessity for accurate enhanced tissue segmentation. However, this segmentation is challenged by many factors. At first, the wall of the LA is very thin. This, when combined with the current limits of CMR spatial resolution, results in the contrast between healthy (non-enhanced) and abnormal (enhanced) left atrial tissue being poorly visualized. Simultaneously, the mean intensity of enhanced regions varies (with the complex response to scan parameters and patient physiology) in unpredictable ways rendering the selection of a signal intensity threshold not so straightforward. In addition, there are few enhanced structures in the proximity of the LA (such as the mitral valve leaflets, the ascending and descending aorta walls, the right atrial wall at the septum, etc) that are not related to left atrial fibrosis or ablation lesion and need to be meticulously distinguished. Likewise, false positives may be also generated by the navigator beam [50], which, in

turn, reduces LGE CMR's ability to visualize abnormal cardiac tissue near the two right pulmonary veins of the LA. To add to the above, the typically irregular heart-rate of AF patients results [51] in (i) ghosting artefacts that further degrade image quality, (ii) failure to accentuate the existent abnormality due to imperfect healthy myocardium nulling. Despite the difficulties in classifying enhanced tissue in the LA, several studies have proposed related techniques. Next, an overview of the previously published approaches is provided.

To begin with, few AF studies [32,41,44] have performed manual segmentation of enhancement by relying on visual perception of experts. However, such an approach is considerably time-consuming and labor-intensive. In addition, it is very difficult to train new technicians to perform this task. Besides, the manual enhancement classification is prone to high intra- and inter-observer variability (even among experts) due to the factors (discussed above) that challenge the enhancement classification and also due to the high degree of patchiness that is characteristic of LGE CMR data-sets of AF patients. As a result, the manual segmentation of enhancement in AF is regarded as a rather unfavourable approach for use in clinical practice.

Motivated by earlier LGE CMR studies [52] on the infarcted left ventricle, a common recipe for segmenting left atrial enhanced tissue in AF patients is using a fixed (i.e., the same for every AF patient) signal intensity threshold expressed in terms of the two basic statistical measures [namely mean value and standard deviation (SD)] of the signal intensity distribution within a reference non-enhanced (healthy) region. With regard to pre-ablation LGE CMR, example reported intensity threshold levels above which a left atrial wall voxel was defined as fibrotic tissue are the three [18] and four [19] SDs above the mean intensity of a region of the left atrial blood-pool (LABP), the two [22] SDs above the mean intensity of a healthy left atrial wall region, and the six [27] SDs above the mean intensity of a region of the left ventricular wall. Analogously, example threshold levels that have been used in post-ablation LGE CMR studies to distinguish between healthy and abnormal tissue are the three [18] SDs above the mean intensity of a region of the LABP, the six [38,42,53] SDs

above the mean intensity of a region of the right ventricular wall, the two [22] and three [11,15,33,35,36,45] SDs above the mean intensity of a healthy left atrial wall region, and the six [27] SDs above the mean intensity of a region of the left ventricular wall. At the same time, other fixed approaches have proposed using 40% [47] and 50% [27] of the maximum left atrial wall intensity as post- and pre-ablation enhancement thresholds, respectively, and also the 50% [27] of the maximum mitral valve intensity as a cut-off level for both pre- and post-ablation enhanced tissue. However, one downside of all these techniques is that they require segmentation of an additional reference region.

To further compensate for the measurement variability due to inter-patient differences (such as body mass index, hematocrit, glomerular filtration rate, etc.), several studies have suggested [13-17,30,46,48,54] to employ a varying (among different patients) threshold level that is benchmarked against the statistics of a healthy region. However, these methods are impeded by lack of automation since the threshold selection for every patient is always decided interactively by an experienced observer. An alternative empirical method [34,37] proposed to use the minimum intensity that eliminated most of the blood-pool pixels in order to acquire a patient-specific enhancement threshold. As well as lack of objectivity and automation, one would expect such an approach to suffer from poor reproducibility all the same. More recently, a method [20] using graph-cuts was brought forward. According to this technique the enhancement segmentation is expressed as a Markov random field energy function minimization problem. However, this method involves a computationally demanding iterative process where hundreds of thousands nodes require processing. As a result, the graph-cuts method does not lend itself well for the real-time direct visualization of left atrial wall tissue destruction.

To summarize, the current situation in the literature is that the computer-aided classification of enhanced tissue in LGE CMR of AF is still an open question, and no algorithm has been deemed clearly better than others [55]. To add to the above, the number of centres that have reported

successful application of LGE CMR to guide clinical AF strategies remains low, while the debate on this technique's diagnostic ability for AF still holds [24,41,53,56].

In this paper, we propose a technique to automatically segment enhanced tissue within the left atrial wall of (pre-ablation and three months post-ablation) LGE CMR data-sets of long-standing persistent AF patients studied at our centre. We employ thresholds that are benchmarked against the statistics of the whole LABP. The test-set cross-validation mechanism is applied to determine the input feature representation and algorithm that best predict enhancement threshold levels. The proposed enhancement classification algorithm was designed to provide the following advantages: (i) Self-regulated classification without requiring expert user interaction, (ii) simplicity to implement allowing fast availability of results, (iii) freedom from intra- and inter-observer variability, (iv) provision of reproducible results, (v) lack of need to manually outline an additional healthy myocardial region, (vi) development was specific to the LA, and (vii) production of realistic estimates regardless mean enhancement intensity and image contrast ratio.

2. Materials and methods

2.1. Study design

Thirteen patients (9 male, 62±11 years old) presented to Royal Brompton Hospital for first-time ablation to treat long-standing persistent drug-refractory AF. 3D LGE CMR data-sets acquired both pre-procedurally and at three months post-ablation were included in this study. We addressed the problem of automatically segmenting left atrial wall enhanced tissue from these data-sets. The image quality was assessed by an expert in CMR. The study was approved by the local (UK) research ethics committee. Written informed consent was obtained from all research participants.

2.2 The ablation procedure

All ablation procedures were performed under general anesthesia. Thoracoscopic bipolar radiofrequency surgical ablation was performed on five consecutive patients. The pulmonary veins were isolated using a clamp and a posterior wall box lesion was created using linear ablation connecting the two superior and inferior veins. The left atrial appendage was excluded in three patients. Percutaneous catheter ablation was delivered on the remaining patients, who underwent a stepwise lesion set strategy: (i) Antral pulmonary vein isolation, (ii) linear ablation at the left atrial roof and mitral isthmus, and (iii) ablation of the left atrial complex fractionated electrograms. Atrial anatomy was reconstructed with the NavX mapping system with an AFocusII catheter (St. Jude Medical, St. Paul, Minnesota, USA). Radiofrequency ablation was performed with a 3.5-mm irrigated-tip catheter (ThermoCool, Biosense Webster, Diamond Bar, California, USA).

2.3 LGE CMR acquisition protocol

CMR was carried out using a Siemens Magnetom Avanto 1.5Tesla scanner (Siemens Medical Systems, Erlangen, Germany). Imaging [57] was performed fifteen minutes after Gd administration (Gadovist - gadobutrol, 0.1mmol/kg body weight, Bayer-Schering, Berlin, Germany) when a transient steady-state of Gd wash-in and wash-out of normal myocardium had been reached. Transverse navigator-gated 3D LGE imaging was performed using a segmented gradient echo sequence as follows: 32 – 36 slices at 1.5mm x 1.5mm x 4mm, reconstructed to 64 – 72 slices at 0.7mm x 0.7mm x 2mm, generalised auto-calibrating partially parallel acquisition (GRAPPA) x2, acquisition window 125ms positioned within the subject-specific rest period, single R-wave gating, chemical shift fat suppression, centric *kz* and centric *ky* ordering, flip angle 20°, crossed-pairs navigator positioned over the dome of the right hemi-diaphragm with nominal navigator acceptance window size of 5mm. The inversion time (TI) used for conventional two-dimensional (2D) breath-hold LGE imaging acquired with alternate R-wave gating was reduced for single R-wave gating by an amount

depending on the patient's heart rate. Nominal acquisition durations were 144 – 160 cardiac cycles, assuming 100% respiratory efficiency.

2.4 The proposed enhancement classification technique

In this section, we describe the work-flow for achieving automatic segmentation of enhancement in LGE CMR data-sets of AF patients studied at our center. In order to assess how well the proposed segmentation technique will generalize in independent (i.e., other than those included in this study) LGE CMR data-sets, we employed the test set cross-validation mechanism [58]. This avenue involved (i) learning the segmentation technique by relying only on a random selection of 3/4 of the study population (training LGE CMR data-sets), and (ii) predicting the responses (enhancement distributions) of the remaining population sub-set (testing LGE CMR data-sets). To improve reliability of future estimations, three rounds of the cross-validation tool were performed.

In pursuance of classifying and isolating AF ablation-related injured tissue and/or pre-existent fibrotic tissue within the left atrial wall, the whole LABP was employed as the reference region. The reason for this choice is that the boundaries of the LABP chamber coincide with the left atrial endocardial surface. Therefore, no extra segmentation step (apart from the left atrial wall segmentation) was required to obtain the specific reference region. Following this selection, intensity I at each left atrial wall voxel i was normalized as

$$NI(i)=[I(i) - \mu_{bp}]/\sigma_{bp} \quad (1)$$

where NI is the normalized intensity and μ_{bp} and σ_{bp} are the mean value and the standard deviation of the signal intensity distribution of the voxels that constitute the LABP.

Next, and with the view to acquiring the "actual" left atrial wall normalized intensity thresholds that mark out the lower boundaries of fibrotic and/or lesion tissue for the "training" data-sets of this study, we relied on an expert observer judgement-based approach. In particular, each of three specialists in LGE CMR was independently shown enhanced tissue classification results

(super-imposed on the LGE CMR data-sets) for normalized intensity cut-off levels that varied from one to six, in steps of 1/8. Subsequently, each expert selected (based on visual perception) the most appropriate threshold level to define enhanced tissue for each data-set (patient). Our objective was to resolve whether a global threshold of normalized intensity would be appropriate for all patients, and if not, to determine the input feature representation and algorithm that best predict the output (i.e., threshold level for enhancement).

The segmentation of the left atrial wall from the LGE CMR data-sets is an integral part of the proposed classification of each left atrial wall voxel as healthy tissue versus fibrotic/injured tissue. In this study, the left atrial wall segmentation (that encompasses the LABP segmentation) was performed semi-automatically. At first, a user-guided level set-based 3D geodesic active contour method [59] was employed to demarcate the left atrial endocardial surface (which coincides with the boundaries of the LABP chamber). This automatic step was subsequently followed by an expert observer manual delineation of the left atrial wall epicardial surface. While performing this non-automatic step, extra care was taken to exclude nearby enhanced structures (such as mitral valve leaflets, aorta walls, and navigator-induced artefacts) not related to left atrial fibrosis or ablation lesion. To account for the intra- and inter-operator variability in this step (due to anatomic variability and partial volume effects), it was arranged to employ a consensus decision-making process. That is to say, the finalized version of every segmented left atrial wall was collaboratively generated by a group of three specialists in CMR of the LA that convened for this purpose. The whole left atrial wall segmentation was carried out using a free open-source segmentation software (ITK-SNAP) [60].

2.5 Analyses

Initially, we aimed at qualitatively evaluating the accuracy of the learnt enhancement segmentation rule on the first-seen (testing) data-sets, by overlaying the enhanced tissue segmentation results upon the original LGE CMR transverse plane slices.

Due to the fact that the segmentation of enhancement in LGE CMR data-sets of AF patients is a complicated task that poses many challenges, the visual assessment of the results based on brightness levels is not alone sufficient. At the same time, both left atrial fibrosis and ablation injury (at three months post-ablation) have been shown [49,61-66] to predict an impairment of atrial conduction/electric activation at the microscopic level. Therefore, there should be a correspondence between the highly current-resistant fibrotic deposits or ablation lesion sets (as these two are visualized by LGE CMR) and regions of low myocardial voltage. In the light of the above and with the view to improving the soundness of the results of this study, we set out to corroborate the proposed LGE CMR enhancement classification technique (apart from using visual inspection criteria based on brightness levels) also by using the unique endocardial bipolar voltage map that was available for one patient of this study and was acquired by a minimally-invasive electro-anatomic mapping (EAM) system. As well as they allow for the indirect assessment of left atrial substrate through voltage tissue characterization, EAM systems [67] also make provision for 3D cardiac chamber reconstruction, accurate navigation in the LA, assessment of adequate energy delivery etc. For this reason, EAM systems are regarded as the linchpin of modern complex AF ablations, and are routinely employed by ~90% of the centres [10].

In addition, we also sought to rate the proposed enhancement segmentation technique: (i) In terms of the measured extent of the left atrial wall structural remodeling (fibrosis). (ii) By looking into the suggested method's capacity for reflecting ablation lesion patterns. To this end, we used 3D volume renderings of the classified enhancement superimposed on the segmented LABP to test the hypothesis that our enhancement segmentation technique (when it is applied to three months post-ablation LGE CMR data-sets) can recreate the (aimed) ablation lesions in a faithful way.

Finally, we investigated how the various threshold levels proposed by other AF studies [18,19] (that also relied on reference regions from within the LABP) fare in LGE CMR data-sets acquired at our center.

3. Results

Four pre-ablation LGE CMR data-sets were excluded by the CMR expert due to poor or non-diagnostic image quality. With regard to the automatic endocardial surface segmentation step, manual editing of the result of the active contour evolution was performed wherever there was a need.

The enhancement normalized intensity thresholds that were selected by the expert observers during the training for pre-ablation and three months post-ablation LGE CMR data-sets are given in Table 1 and Table 2, respectively. From these results, global thresholds of $T_{PRE} = 1\ 1/4$ (for pre-ablation LGE CMR data-sets) and $T_{POST} = 1\ 5/8$ (for data-sets acquired at three months post-ablation) best predict enhanced tissue for AF patients studied at our center. The three cross-validation rounds produced similar results. Therefore, these threshold levels were used for all further analyses.

A qualitative evaluation of the predictive power of the chosen thresholds on first-seen (testing) LGE CMR data-sets is provided in Fig. 1 and Fig. 2, where the enhanced tissue segmentation results have been overlaid upon the original transverse plane slices of "testing" LGE CMR data-sets. It was generally observed that the proposed thresholds resulted in enhancement classifications that are in good concordance with visual perception for both pre-ablation (baseline) and three months post-ablation data-sets.

An additional substantiation of our segmentation method against the unique endocardial bipolar voltage map that was available for one patient of this study is demonstrated in Fig. 3. A visually appreciable correlation between left atrial regions of classified fibrotic deposit (in a pre-ablation LGE CMR) and areas of low (i.e., $< 0.5\text{mV}$) bipolar endocardial voltage can be seen.

By surveying the baseline scans of this study, we found that the mean relative extent of the measured native fibrosis associated with AF was 26.14 ± 11.17 % (Fig. 4, Table 3). This figure falls within the expected [13] range for the specific arrhythmia phenotype.

The 3D visualization of the three months post-ablation LGE CMR data-sets of this study showed that the revealed distributions of classified enhancement typically emulated the ablation lesion patterns (acquired after implementing the ablation strategies described in Section 2.2). A representative example is shown in Fig. 5, where (the 3D volume rendering of) the classified enhancement distribution comprises encirclement of each ipsilateral pair of pulmonary veins at their antra, as well as a linear pattern at the mitral isthmus.

As an interim summary, the results presented up to this point allowed us to reach the decision that any left atrial wall voxel i with normalized intensity $NI(i)$ above $T_{PRE} = 1 \frac{1}{4}$ in a baseline scan is defined as abnormal native fibrotic tissue, whereas any left atrial wall voxel i with normalized intensity $NI(i)$ above $T_{POST} = 1 \frac{5}{8}$ in a three months post-ablation scan is classified as abnormal native fibrotic or AF ablation-related injured tissue.

Finally, comparisons of the proposed enhancement segmentation technique with other related papers [18,19] that suggested using different threshold levels for segmenting enhancement in LGE CMR data-sets of AF patients are shown in Fig. 6 and Fig. 7. The figures illustrate that, when it comes to LGE CMR data-sets acquired to our centre, our proposed thresholds conspicuously outperform those proposed in studies cited in [18] and [19].

4. Discussion - conclusions

4.1 The main contribution

AF represents a major public health problem. Putting this abnormal heart condition in the disease rates comparison context, today everyone aged forty or over has a lifetime risk of

developing AF of at least one in four, compared, for example, with one in eight for breast cancer in women of the same age group [68,69]. On top of this, the AF prevalence is expected [3] to double by 2050. Ablation treatment of AF is associated with modest outcomes. In order for LGE CMR to ameliorate the AF management, the ready availability of the accurate enhancement segmentation is required. However, the computer-aided classification of enhanced tissue in LGE CMR of AF is still an open question. This study was designed to retrospectively propose a fast automatic method that reliably distinguishes enhanced (abnormal) from non-enhanced (healthy) tissue within the left atrial wall of (baseline and three months post-ablation) LGE CMR data-sets of long-standing persistent AF patients studied at our centre. Detection and isolation of enhancement was achieved by employing thresholds benchmarked against the statistics of the entire LABP. On the whole, global normalized intensity threshold levels $T_{PRE}=1 \frac{1}{4}$ and $T_{POST}=1 \frac{5}{8}$ were found to segment enhancement in data-sets acquired pre-ablation and at three months post-ablation, respectively. The proposed segmentation algorithm combines the following advantages: (i) It is self-regulated without requiring expert user interaction, (ii) it is simple to implement, and runs in a couple of seconds on a typical PC allowing fast availability of results, (iii) it eliminates observer bias, (iv) it provides reproducible results, (v) it does not require manual outlining of an additional healthy myocardial region, (vi) it has been developed particularly for the LA, (vii) it produces realistic estimates regardless mean enhancement intensity and image contrast ratio.

The predictive power of the proposed enhancement segmentation rule was verified on first-seen (testing) LGE CMR data-sets through the cross-validation mechanism. This tool allows for minimally biased results (by preserving the total blinding of the testing data-sets from the training procedure), while at the same time uses the available data as effectively as possible. Apart from corroborating the segmentation results by relying on visual inspection of LGE CMR brightness levels, we also verified the proposed technique by using the unique endocardial bipolar voltage map that was available for one patient of this study. The observation of a marked correspondence between

the fibrotic deposits (classified by our segmentation technique) and regions of low myocardial voltage (measured with an EAM system) boosts further the employment of non-invasive LGE CMR in clinical practice as a guidance tool on left atrial substrate characterization. In addition, by measuring the extent of classified fibrosis and correlating it with the studied arrhythmia phenotype, we showed that the proposed segmentation technique favours the settlement of the link between the degree of fibrosis and the disease severity in AF [13]. This type of measurement is also key for noninvasively identifying patients that are unlikely to benefit from ablation. Furthermore, the suggested method's capacity for reflecting the expected ablation lesion patterns was demonstrated by using 3D volume rendering techniques. Such knowledge could prove useful in pinpointing ablation line gaps and guiding repeat operations. All in all, the proposed segmentation technique: (i) Has great potential for successful employment in the AF management within our centre, and (ii) provides a highly desirable (according to the present status of the related literature) validation of the LGE CMR technique for AF studies.

4.2 Global versus patient-specific thresholding

LGE CMR data-sets from AF patients are highly variable with respect to image noise, contrast, and mean enhancement intensity. To address this problem, some studies [20] have suggested employing a patient-specific (rather than a fixed) threshold level. However, we found in this study that the selected fixed threshold levels applied well to all LGE CMR data-sets regardless image contrast ratio and mean enhancement intensity. A possible explanation for this is that the normalization of the left atrial wall intensities (against the statistics of the signal intensity distribution of the voxels that constitute the LABP in the same data-set) appears to have compensated for the contrast and mean enhancement intensity variability.

4.3 Enhancement segmentation: post-ablation as opposed to pre-ablation data-sets

In this study, there was a sense of greater confidence in the segmentation results of post-ablation rather than baseline LGE CMR data-sets. This is in accordance with the surrounding circumstances since the native pre-existent fibrosis is known [26] to have a more diffuse distribution, as opposed to the iatrogenic scarring which exhibits a focal pattern. However, the three months post-ablation LGE CMR data-sets of AF patients are expected to involve enhancement that corresponds to both native fibrotic tissue and radiofrequency energy application lesion sets. It is our opinion that at the moment it is very challenging to distinguish between these two types of enhancement that reside on a post-ablation data-set, despite the fact that the pre-procedural data-sets are also available for these patients. The reasons for this are (i) the inaccessible/unpredictable intensity scaling (that takes place within the MR scanner before exporting the data) which results in the two types of enhancement having arbitrary and possibly common intensities, and (ii) the two types of enhancement are contiguous. Finally, it only makes things worse the fact that these two sources of enhancement sit at the opposite ends of a ring diameter and snarl at each other, since AF-related fibrosis has been postulated to be a central component of arrhythmia maintenance, while, on the other hand, ablation-related scar aims at favouring freedom of arrhythmia.

4.4 Left atrial wall segmentation

Segmentation of the left atrial wall is a crucial step before segmenting enhancement. The consensus manual delineation of the left atrial wall epicardial border is a downside of this study, as it is a time-consuming step taking up to one hour. Our decision to implement this step manually was based on the fact that fully automatic approaches at the moment result in unreliable left atrial wall segmentations and, as a result, they require significant manual feedback. In any case, this paper is concerned only with the classification of enhancement within the left atrial wall of AF patients; the determination of the left atrial wall boundaries is beyond the scope of this study. Even though our proposed enhancement classification technique was applied to left atrial walls that had been

segmented semi-automatically, it could also be executed with no modification within fully automatically segmented left atrial walls.

4.5 Comparison with other papers

Another contribution of this paper is that we compare our technique with other related approaches that proposed different threshold levels (although they also relied on reference regions from within the LABP) for segmenting enhancement in LGE CMR data-sets of AF patients. The failure of threshold levels suggested by other papers was illustrated for data-sets acquired in our centre. A reason for this discrepancy may be the inter-centre variability in CMR acquisition parameters, such as the optimal timing of imaging after contrast administration, choice and ideal dosage of contrast agent, selection of the best TI etc. Another possibility is that the differences in the proposed thresholds arose out of regional variation in the reference region statistics. In particular, whereas this study employed the whole LABP, segmented directly for the LGE CMR image, the other two papers segmented the LABP from the 3D magnetic resonance angiography (MRA) sequence, and then registered this segmentation with the LGE CMR image. Finally, to account for the inherent spatial error (that occurred in the process of registering the non-electrocardiography-gated MRA sequence with the electrocardiography and respiratory motion gated free-breathing LGE sequence), the authors of [18] and [19] concluded their reference region by performing mathematical morphology shrinkage. Therefore, their reference region was most likely a smaller sub-region within the most central part of the LABP which (in our LGE CMR data-sets) was observed (Fig. 8) to have significantly different statistic measures (standard deviation) from the entire LABP.

To summarize, threshold levels employed by other centres may not be usable for clinical studies performed in our centre; instead, the operator would have to resort to threshold re-adjustment in order to achieve accurate assessment of left atrial substrate, and prevent unnecessary ablation. Inter-centre differences in the CMR acquisition protocol and image analysis strategy

inevitably impede the selection of a universally optimal algorithm for segmentation of enhancement in AF studies.

4.6 Other limitations of this study

The major limitation of this study was the relatively small sample size. Therefore, further larger studies are required to confirm these results. Furthermore, only one voltage map was available for validation. Another limitation of this paper is that few of the criteria used to assess the proposed technique are qualitative, mainly due to the lack of a reliable gold standard ground truth. While qualitative criteria have been rich in communicating the message, it is recognized, at the same time, that quantitative tools would have allowed for much greater precision and objectiveness in comparisons.

4.7 In conclusion

We proposed a method to distinguish enhanced (abnormal) from non-enhanced (healthy) tissue within the left atrial wall of (pre-ablation and 3 months post-ablation) LGE CMR data-sets from long-standing persistent AF patients studied at our centre. Segmentation of enhancement was achieved by employing thresholds benchmarked against the statistics of the whole LABP. Global normalized intensity threshold levels $T_{PRE}=1 \frac{1}{4}$ and $T_{POST}=1 \frac{5}{8}$ were found to segment enhancement in data-sets acquired pre-ablation and at three months post-ablation, respectively. The proposed segmentation algorithm combines the following advantages: (i) It is self-regulated, (ii) it is simple to implement allowing fast availability of results, (iii) it eliminates observer bias, (iv) it provides reproducible results, (v) it does not require manual outlining of an additional healthy myocardial region, (vi) it has been developed particularly for the left atrium, (vii) it produces realistic estimates regardless mean enhancement intensity and image contrast ratio. The segmentation results were corroborated by relying on visual inspection of brightness levels of LGE CMR images and

one endocardial bipolar voltage map. The measured extent of pre-ablation fibrosis fell within the normal range for the specific arrhythmia phenotype. 3D volume renderings of segmented post-ablation enhancement emulated the expected ablation lesion patterns. The proposed technique has great potential for successful employment in the AF management within our centre. The results provide a highly desirable (according to the present status of the related literature) validation of the LGE CMR technique for AF studies. The cut-off levels employed by other centres may not be usable for clinical studies performed in our centre. Inter-centre differences in the CMR acquisition protocol and image analysis strategy inevitably impede the selection of a universally optimal algorithm for segmentation of enhancement in AF studies. Further larger studies are required to confirm the results of this paper.

5. Competing interests

DJP is a consultant for Siemens, and a stockholder and director of Cardiovascular Imaging Solutions Ltd. The other authors have no competing interests to declare.

6. Authors' contributions

AG contributed to the design of this study, carried out the data analysis and data interpretation, and drafted the manuscript. EN participated in the data analysis and CMR data acquisition. JK designed the CMR sequence, participated in the data analysis, and helped to draft the manuscript. IP participated in the data analysis and helped to draft the manuscript. ISH contributed to the data analysis. SH participated in the study design, and electro-physiology and CMR data acquisition. DJP contributed to the conception of the study and helped to draft the manuscript. RM participated in the data analysis, and helped with the design and conception of this study. TW

participated in the conception of this study, as well as in the electro-physiology data acquisition. DNF contributed to design and the conception of this study. All authors read and approved the final manuscript.

7. Acknowledgements

This work was supported by funds from the NIHR Cardiovascular Biomedical Research Unit of Royal Brompton & Harefield NHS Foundation Trust and Imperial College London.

8. References

- [1] Kostin S, Klein G, Szalay Z, Hein S, Bauer EP, Schaper J. Structural correlate of atrial fibrillation in human patients. *Cardiovascular Research* 2002;**54**(2):361–379.
- [2] Boldt A, Wetzel U, Lauschke J, Weigl J, Gummert J, Hindricks G, Kottkamp H, Dhein S. Fibrosis in left atrial tissue of patients with atrial fibrillation with and without underlying mitral valve disease. *Heart* 2004;**90**(4):400–405.
- [3] Appelbaum E, Manning WJ. Left atrial fibrosis by late gadolinium enhancement cardiovascular magnetic resonance predicts recurrence of atrial fibrillation after pulmonary vein isolation: Do you see what I see? *Circulation: Arrhythmia and Electrophysiology* 2014;**7**(1):2–4.
- [4] Stewart S, Hart CL, Hole DJ, McMurray JJ. A population-based study of the long- term risks associated with atrial fibrillation: 20-year follow-up of the Renfrew/Paisley study. *American Journal Medicine* 2002;**113**(5):359–364.
- [5] Wolf PA, Abbott RD, Kannel WB. Atrial fibrillation as an independent risk factor for stroke: The Framingham study. *Stroke* 1991;**22**(8):983–988.

- [6] January CT, Wann LS, Alpert JS, Calkins H, Cigarroa JE, Cleveland JC, Conti JB, Ellinor PT, Ezekowitz MD, Field ME, Murray KT, Sacco RL, Stevenson WG, Tchou PJ, Tracy CM, Yancy CW. 2014
AHA/ACC/HRS guideline for the management of patients with atrial fibrillation: executive summary: a report of the American College of Cardiology/American Heart Association task force on practice guidelines and the Heart Rhythm society. *Journal of the American College of Cardiology* 2014;**64**(21):2246–2280.
- [7] Cappato R, Calkins H, Chen SA, Davies W, Iesaka Y, Kalman J, Kim YH, Klein G, Packer D, Skanes A. Worldwide survey on the methods, efficacy, and safety of catheter ablation for human atrial fibrillation. *Circulation* 2005;**111**(9):1100–1105.
- [8] Ouyang F, Tilz R, Chun J, Schmidt B, Wissner E, Zerm T, Neven K, Köktürk B, Konstantinidou M, Metzner A, Fuernkranz A, Kuck KH. Long-term results of catheter ablation in paroxysmal atrial fibrillation: Lessons from a 5-year follow-up. *Circulation* 2010;**122**(23):2368–2377.
- [9] Weerasooriya R, Khairy P, Litalien J, Macle L, Hocini M, Sacher F, Lellouche N, Knecht S, Wright M, Nault I, Miyazaki S, Scavee C, Clementy J, Haissaguerre M, Jais P. Catheter ablation for atrial fibrillation: are results maintained at 5 years of follow-up? *Journal of the American College of Cardiology* 2011;**57**(2):160–166.
- [10] Calkins H, Kuck KH, Cappato R, Brugada J, Camm AJ, Chen S-A, Crijns HJG, Damiano Jr. RJ, Davies DW, DiMarco J, Edgerton J, Ellenbogen K, Ezekowitz MD, Haines DE, Haissaguerre M, Hindricks G, Iesaka Y, Jackman W, Jalife J, Jais P, Kalman J, Keane D, Kim Y-H, Kirchhof P, Klein G, Kottkamp H, Kumagai K, Lindsay BD, Mansour M, Marchlinski FE, McCarthy PM, Mont JL, Morady F, Nademanee K, Nakagawa H, Natale A, Nattel S, Packer DL, Pappone C, Prystowsky E, Raviele A, Reddy V, Ruskin JN, Shemin RJ, Tsao H-M, Wilber D. 2012 HRS/EHRA/ECAS expert consensus statement on catheter and surgical ablation of atrial fibrillation: Recommendations for patient selection, procedural techniques, patient management and follow-up, definitions, endpoints, and research trial design. *Heart Rhythm* 2012;**9**(4):632–696.

- [11] Badger TJ, Oakes RS, Daccarett M, Burgon NS, Akoum N, Fish EN, Blauer JJ, Rao SN, Adjei-Poku Y, Kholmovski EG, Vijayakumar S, Di Bella EV, MacLeod RS, Marrouche NF. Temporal left atrial lesion formation after ablation of atrial fibrillation. *Heart Rhythm* 2009;**6**(2):161–168.
- [12] Kim RJ, Wu E, Rafael A, Chen EL, Parker MA, Simonetti O, Klocke FJ, Bonow RO, Judd RM. The use of contrast-enhanced magnetic resonance imaging to identify reversible myocardial dysfunction. *The New England Journal of Medicine* 2000;**343**(20):1445–1453.
- [13] Oakes RS, Badger TJ, Kholmovski EG, Akoum N, Burgon NS, Fish EN, Blauer JJ, Rao SN, DiBella EV, Segerson NM, Daccarett M, Windfelder J, McGann CJ, Parker D, MacLeod RS, Marrouche NF. Detection and quantification of left atrial structural remodeling with delayed-enhancement magnetic resonance imaging in patients with atrial fibrillation. *Circulation* 2009;**119**(13):1758–1767.
- [14] Mahnkopf C, Badger TJ, Burgon NS, Daccarett M, Haslam TS, Badger CT, McGann CJ, Akoum N, Kholmovski E, Macleod RS, Marrouche NF. Evaluation of the left atrial substrate in patients with lone atrial fibrillation using delayed-enhanced MRI: Implications for disease progression and response to catheter ablation. *Heart Rhythm* 2010;**7**(10):1475–1481.
- [15] Akoum N, Daccarett M, McGann C, Segerson N, Vergara G, Kuppahally S, Badger T, Burgon N, Haslam T, Kholmovski E, Macleod R, Marrouche N. Atrial fibrosis helps select the appropriate patient and strategy in catheter ablation of atrial fibrillation: a DE-MRI guided approach. *Journal of Cardiovascular Electrophysiology* 2011;**22**(1):16–22.
- [16] Vergara GR, Marrouche NF. Tailored management of atrial fibrillation using a LGE-MRI based model: From the clinic to the electrophysiology laboratory. *Journal of Cardiovascular Electrophysiology* 2011;**22**(4):481–487.
- [17] Daccarett M, Badger TJ, Akoum N, Burgon NS, Mahnkopf C, Vergara G, Kholmovski E, McGann CJ, Parker D, Brachmann J, Macleod RS, Marrouche NF. Association of left atrial fibrosis detected by delayed-enhancement magnetic resonance imaging and the risk of stroke in patients with atrial fibrillation. *Journal of the American College of Cardiology* 2011;**57**(7):831–838.

- [18] Malcolme-Lawes LC, Juli C, Karim R, Bai W, Quest R, Lim PB, Jamil-Copley S, Kojodjojo P, Ariff B, Davies DW, Rueckert D, Francis DP, Hunter R, Jones D, Boubertakh R, Petersen SE, Schilling R, Kanagaratnam P, Peters NS. Automated analysis of atrial late gadolinium enhancement imaging that correlates with endocardial voltage and clinical outcomes: A 2-center study. *Heart Rhythm* 2013;**10**(8):1184–1191.
- [19] Ravanelli D, dal Piaz EC, Centonze M, Casagrande G, Marini M, Del Greco M, Karim R, Rhode K, Valentini A. A novel skeleton based quantification and 3-D volumetric visualization of left atrium fibrosis using late gadolinium enhancement magnetic resonance imaging. *IEEE Transactions on Medical Imaging* 2014;**33**(2):566–576.
- [20] Karim R, Arujuna A, Housden RJ, Gill J, Cliffe H, Matharu K, Gill J, Rindaldi CA, O'Neill M, Rueckert D, Razavi R, Schaeffter T, Rhode K. A method to standardize quantification of left atrial scar from delayed-enhancement MR images. *IEEE Journal of Translational Engineering in Health and Medicine* 2014;doi: 10.1109/JTEHM.2014.2312191.
- [21] Jadidi AS, Cochet H, Shah AJ, Kim SJ, Duncan E, Miyazaki S, Sermesant M, Lehrmann H, Lederlin M, Linton N, Forclaz A, Nault I, Rivard L, Wright M, Liu X, Scherr D, Wilton SB, Roten L, Pascale P, Derval N, Sacher F, Knecht S, Keyl C, Hocini M, Montaudon M, Laurent F, Haïssaguerre M, Jaïs P. Inverse relationship between fractionated electrograms and atrial fibrosis in persistent atrial fibrillation: combined magnetic resonance imaging and high-density mapping. *Journal of the American College of Cardiology* 2013;**62**(9):802–812.
- [22] Kapa S, Desjardins B, Callans DJ, Marchlinski FE, Dixit S. Contact electroanatomic mapping derived voltage criteria for characterizing left atrial scar in patients undergoing ablation for atrial fibrillation. *Journal of Cardiovascular Electrophysiology* 2014;**25**(10):1044–1052.
- [23] McGann C, Akoum N, Patel A, Kholmovski E, Revelo P, Damal K, Wilson B, Cates J, Harrison A, Ranjan R, Burgon NS, Greene T, Kim D, DiBella EVR, Parker D, MacLeod RS, Marrouche NF. Atrial

fibrillation ablation outcome is predicted by left atrial remodeling on MRI. *Circulation: Arrhythmia and Electrophysiology* 2014;**7**(1):23–30.

[24] Sramko M, Peichl P, Wichterle D, Tintera J, Weichet J, Maxian R, Pasnisinova S, Kockova R, Kautzner J. Clinical value of assessment of left atrial late gadolinium enhancement in patients undergoing ablation of atrial fibrillation. *International Journal of Cardiology* 2015;**179**:351–357.

[25] Akkaya M, Marrouche N, Higuchi K, Koopmann M, Damal K, Kholmovski E, McGann C. The degree of left atrial structural remodeling impacts left ventricular ejection fraction in patients with atrial fibrillation. *Archives of the Turkish Society of Cardiology* 2014;**42**(1):11–19.

[26] Fukumoto K, Habibi M, Gucuk Ipek E, Khurram IM, Zimmerman SL, Zipunnikov V, Spragg DD, Ashikaga H, Rickard J, Marine JE, Berger RD, Calkins H, Nazarian S. Comparison of pre-existing versus ablation-induced late gadolinium enhancement on left atrial magnetic resonance imaging. *Heart Rhythm*, Accepted manuscript –in press, doi: 10.1016/j.hrthm.2014.12.021.

[27] Hwang SH, Oh YW, Lee DI, Shim J, Park SW, Kim YH. Evaluation of quantification methods for left atrial late gadolinium enhancement based on different references in patients with atrial fibrillation. *International Journal of Cardiovascular Imaging*, Accepted manuscript –in press, doi: 10.1007/s10554-014-0563-0.

[28] Khurram IM, Beinart R, Zipunnikov V, Dewire J, Yarmohammadi H, Sasaki T, Spragg DD, Marine JE, Berger RD, Halperin HR, Calkins H, Zimmerman SL, Nazarian S: Magnetic resonance image intensity ratio, a normalized measure to enable interpatient comparability of left atrial fibrosis. *Heart Rhythm* 2014;**11**(1):85–92.

[29] Dewire J, Khurram IM, Pashakhanloo F, Spragg D, Marine JE, Berger RD, Ashikaga H, Rickard J, Zimmerman SL, Zipunnikov V, Calkins H, Nazarian S. The association of pre-existing left atrial fibrosis with clinical variables in patients referred for catheter ablation of atrial fibrillation. *Clinical Medicine Insights: Cardiology* 2014;**8**(Suppl 1):25–30.

- [30] Cochet H, Mouries A, Nivet H, Sacher F, Derval N, Denis A, Merle M, Relan J, Hocini M, Haissaguerre M, Laurent F, Montaudon M, Jais P. Age, atrial fibrillation, and structural heart disease are the main determinants of left atrial fibrosis detected by delayed-enhanced magnetic resonance imaging in a general cardiology population. *Journal of Cardiovascular Electrophysiology*, online early view before inclusion in an issue, doi:10.1111/jce.12651.
- [31] Peters DC, Wylie JV, Hauser TH, Kissinger KV, Botnar RM, Essebag V, Josephson ME, Manning WJ. Detection of pulmonary vein and left atrial scar after catheter ablation with three-dimensional navigator-gated delayed enhancement MR imaging: Initial experience. *Radiology* 2007;**243**(3):690–695.
- [32] Reddy VY, Schmidt EJ, Holmvang G, Fung M. Arrhythmia recurrence after atrial fibrillation ablation: Can magnetic resonance imaging identify gaps in atrial ablation lines? *Journal of Cardiovascular Electrophysiology* 2008;**19**(4):434–437.
- [33] McGann CJ, Kholmovski EG, Oakes RS, Blauer JJ, Daccarett M, Segerson N, Airey KJ, Akoum N, Fish E, Badger TJ, DiBella EV, Parker D, MacLeod RS, Marrouche NF. New magnetic resonance imaging-based method for defining the extent of left atrial wall injury after the ablation of atrial fibrillation. *Journal of the American College of Cardiology* 2008;**52**(15):1263–1271.
- [34] Peters DC, Wylie JV, Hauser TH, Nezafat R, Han Y, Woo JJ, Taclas J, Kissinger KV, Goddu B, Josephson ME, Manning WJ. Recurrence of atrial fibrillation correlates with the extent of post-procedural late gadolinium enhancement: A pilot study. *Journal of the American College of Cardiology: Cardiovascular Imaging* 2009;**2**(3):308–316.
- [35] Segerson NM, Daccarett M, Badger TJ, Shabaan A, Akoum N, Fish EN, Rao S, Burgon NS, Adjei-Poku Y, Kholmovski E, Vijayakumar S, DiBella EV, MacLeod RS, Marrouche NF. Magnetic resonance imaging-confirmed ablative debulking of the left atrial posterior wall and septum for treatment of persistent atrial fibrillation: Rationale and initial experience. *Journal of Cardiovascular Electrophysiology* 2010;**21**(2):126–32.

- [36] Badger TJ, Daccarett M, Akoum NW, Adjei-Poku YA, Burgon NS, Haslam TS, Kalvaitis S, Kuppahally S, Vergara G, McMullen L, Anderson PA, Kholmovski E, MacLeod RS, Marrouche NF. Evaluation of left atrial lesions after initial and repeat atrial fibrillation ablation: Lessons learned from delayed-enhancement MRI in repeat ablation procedures. *Circulation: Arrhythmia and Electrophysiology* 2010;**3**(3):249–259.
- [37] Taclas JE, Nezafat R, Wylie JV, Josephson ME, Hsing J, Manning WJ, Peters DC. Relationship between intended sites of RF ablation and post-procedural scar in AF patients, using late gadolinium enhancement cardiovascular magnetic resonance. *Heart Rhythm* 2010;**7**(4):489–496.
- [38] Knowles BR, Caulfield D, Cooklin M, Rinaldi CA, Gill J, Bostock J, Razavi R, Schaeffter T, Rhode KS. 3-D visualization of acute RF ablation lesions using MRI for the simultaneous determination of the patterns of necrosis and edema. *IEEE Transactions on Biomedical Engineering* 2010;**57**(6):1467–1475.
- [39] McGann C, Kholmovski E, Blauer J, Vijayakumar S, Haslam T, Cates J, DiBella E, Burgon N, Wilson B, Alexander A, Prastawa M, Daccarett M, Vergara G, Akoum N, Parker D, MacLeod R, Marrouche N. Dark regions of no-reflow on late gadolinium enhancement magnetic resonance imaging result in scar formation after atrial fibrillation ablation. *Journal of the American College of Cardiology* 2011;**58**(2):177–185.
- [40] Vergara GR, Vijayakumar S, Kholmovski EG, Blauer JJ, Guttman MA, Gloschat C, Payne G, Vij K, Akoum NW, Daccarett M, McGann CJ, Macleod RS, Marrouche NF. Real-time magnetic resonance imaging-guided radiofrequency atrial ablation and visualization of lesion formation at 3 Tesla. *Heart Rhythm* 2011;**8**(2):295–303.
- [41] Spragg DD, Khurram I, Zimmerman SL, Yarmohammadi H, Barcelon B, Needleman M, Edwards D, Marine JE, Calkins H, Nazarian S. Initial experience with magnetic resonance imaging of atrial scar and co-registration with electroanatomic voltage mapping during atrial fibrillation: Success and limitations. *Heart Rhythm* 2012;**9**(12):2003–2009.

- [42] Arujuna A, Karim R, Caulfield D, Knowles B, Rhode K, Schaeffter T, Kato B, Rinaldi CA, Cooklin M, Razavi R, O'Neill MD, Gill J. Acute pulmonary vein isolation is achieved by a combination of reversible and irreversible atrial injury after catheter ablation: Evidence from magnetic resonance imaging. *Circulation: Arrhythmia and Electrophysiology* 2012;**5**(4):691–700.
- [43] Ranjan R, Kholmovski EG, Blauer J, Vijayakumar S, Volland NA, Salama ME, Parker DL, Macleod R, Marrouche NF. Identification and acute targeting of gaps in atrial ablation lesion sets using a real time MRI system. *Circulation Arrhythmia and Electrophysiology* 2012;**5**(6):1130–1135.
- [44] Sohns C, Karim R, Harrison J, Arujuna A, Linton N, Sennett R, Lambert H, Leo G, Williams S, Razavi R, Wright M, Schaeffter T, O'Neill M, Rhode K. Quantitative magnetic resonance imaging analysis of the relationship between contact force and left atrial scar formation after catheter ablation of atrial fibrillation. *Journal of Cardiovascular Electrophysiology* 2014;**25**(2):138–145.
- [45] Parmar BR, Jarrett TR, Burgon NS, Kholmovski EG, Akoum NW, Hu N, Macleod RS, Marrouche NF, Ranjan R. Comparison of left atrial area marked ablated in electroanatomical maps with scar in MRI. *Journal of Cardiovascular Electrophysiology* 2014;**25**(5):457–463.
- [46] Wylie JV Jr, Peters DC, Essebag V, Manning WJ, Josephson ME, Hauser TH. Left atrial function and scar after catheter ablation of atrial fibrillation. *Heart Rhythm* 2008;**5**(5):656–662.
- [47] Bisbal F, Guiu E, Cabanas-Grandio P, Berruezo A, Prat-Gonzalez S, Vidal B, Garrido C, Andreu D, Fernandez-Armenta J, Tolosana JM, Arbelo E, de Caralt TM, Perea RJ, Brugada J, Mont L: CMR-guided approach to localize and ablate gaps in repeat AF ablation procedure. *JACC: Cardiovascular Imaging* 2014;**7**(7):653–663.
- [48] Higuchi K, Akkaya M, Akoum N, Marrouche NF. Cardiac MRI assessment of atrial fibrosis in atrial fibrillation: Implications for diagnosis and therapy. *Heart* 2014;**100**(7):590–596.
- [49] Harrison JL, Jensen HK, Peel SA, Chiribiri A, Grøndal AK, Bloch LØ, Pedersen SF, Bentzon JF, Kolbitsch C, Karim R, Williams SE, Linton NW, Rhode KS, Gill J, Cooklin M, Rinaldi CA, Wright M, Kim WY, Schaeffter T, Razavi RS, O'Neill MD. Cardiac magnetic resonance and electroanatomical mapping

of acute and chronic atrial ablation injury: A histological validation study. *European Heart Journal* 2014;**35**(22):1486–1495.

[50] Keegan J, Drivas P, Firmin DN. Navigator artifact reduction in three-dimensional late gadolinium enhancement imaging of the atria. *Magnetic Resonance in Medicine* 2014;**72**(3):779–785.

[51] Weingärtner S, Akçakaya M, Basha T, Kissinger KV, Goddu B, Berg S, Manning WJ, Nezafat R. Combined saturation/inversion recovery sequences for improved evaluation of scar and diffuse fibrosis in patients with arrhythmia or heart rate variability. *Magnetic Resonance in Medicine* 2014;**71**(3):1024–1034.

[52] Kolipaka A, Chatzimavroudis GP, White RD, O'Donnell TP, Setser RM. Segmentation of non-viable myocardium in delayed enhancement magnetic resonance images. *International Journal of Cardiovascular Imaging* 2005;**21**(2-3):303–311.

[53] Hunter RJ, Jones DA, Boubertakh R, Malcolme-Lawes LC, Kanagaratnam P, Juli CF, Davies DW, Peters NS, Baker V, Earley MJ, Sporton S, Davies LC, Westwood M, Petersen SE, Schilling RJ. Diagnostic accuracy of cardiac magnetic resonance imaging in the detection and characterization of left atrial catheter ablation lesions: A multicenter experience. *Journal of Cardiovascular Electrophysiology* 2013;**24**(4):396–403.

[54] Akkaya M, Higuchi K, Koopmann M, Burgon N, Erdogan E, Damal K, Kholmovski E, McGann C, Marrouche NF. Relationship between left atrial tissue structural remodelling detected using late gadolinium enhancement MRI and left ventricular hypertrophy in patients with atrial fibrillation. *Europace* 2013;**15**(12):1725–1732.

[55] Karim R, Housden RJ, Balasubramaniam M, Chen Z, Perry D, Uddin A, Al-Beyatti Y, Palkhi E, Acheampong P, Obom S, Hennemuth A, Lu YL, Bai W, Shi W, Gao Y, Peitgen H-O, Radau P, Razavi R, Tannenbaum A, Rueckert D, Cates J, Schaeffter T, Peters D, MacLeod R, Rhode K. Evaluation of current algorithms for segmentation of scar tissue from late gadolinium enhancement cardiovascular

magnetic resonance of the left atrium: An open-access grand challenge. *Journal of Cardiovascular Magnetic Resonance* 2013;**15**(1):105.

[56] Harrison JL, Sohns C, Linton NW, Karim R, Williams SE, Rhode KS, Gill J, Cooklin M, Rinaldi CA, Wright M, Schaeffter T, Razavi RS, O'Neill MD. Repeat left atrial catheter ablation: Cardiac magnetic resonance prediction of endocardial voltage and gaps in ablation lesion sets. *Circulation: Arrhythmia and Electrophysiology* (published online before print), doi: 10.1161/CIRCEP.114.002066.

[57] Keegan J, Jhooti J, Babu-Narayan SV, Drivas P, Ernst S, Firmin DN. Improved respiratory efficiency of 3D late gadolinium enhancement imaging using the continuously adaptive windowing strategy (CLAWS). *Magnetic Resonance in Medicine* 2014;**71**(3):1064–1074.

[58] Geisser S. Predictive Inference: An Introduction. New York, NY: Chapman and Hall, Inc. ISBN: 0-412-03471-9, 1993.

[59] Caselles V, Kimmel R, Sapiro G. Geodesic active contours. *International Journal of Computer Vision* 1997;**22**(1):61–79.

[60] Yushkevich PA, Piven J, Hazlett HC, Smith RG, Ho S, Gee JC, Gerig G. User-guided 3D active contour segmentation of anatomical structures: Significantly improved efficiency and reliability. *Neuroimage* 2006;**31**(3):1116–1128.

[61] Kucera JP, Rudy Y. Mechanistic insights into very slow conduction in branching cardiac tissue. A model study. *Circulation Research* 2001;**89**(9):799–806.

[62] Jacquemet V, Henriquez CS. Genesis of complex fractionated atrial electrograms in zones of slow conduction: A computer model of microfibrosis. *Heart Rhythm* 2009;**6**(6):803–810.

[63] Comtois P, Nattel S. Interactions between cardiac fibrosis spatial pattern and ionic remodeling on electrical wave propagation. In the *Proceedings of the 33rd Annual International Conference of the IEEE Engineering in Medicine and Biology Society (EMBS 2011)*. Boston, Massachusetts, USA, August 30 - September 3, 2011:4669–4672.

- [64] McDowell KS, Vadakkumpadan F, Blake R, Blauer J, Plank G, MacLeod RS, Trayanova NA. Methodology for patient-specific modeling of atrial fibrosis as a substrate for atrial fibrillation. *Journal of Electrocardiology* 2012;**45**(6):640–645.
- [65] Zhao J, Stephenson RS, Sands GB, LeGrice IJ, Zhang H, Jarvis JC, Smaill BH. Atrial fibrosis and atrial fibrillation: a computer simulation in the posterior left atrium. *Functional Imaging and Modeling of the Heart 2013 (FIMH 2013)*. S. Ourselin, D. Rueckert, and N. Smith (Eds.), Lecture Notes Computer Science (LNCS) 7945, pp. 400–408, Springer-Verlag Berlin Heidelberg, 2013.
- [66] Campos FO, Wiener T, Prassl AJ, dos Santos RW, Sánchez-Quintana D, Ahammer H, Plank G, Hofer E. Electro-anatomical characterization of atrial microfibrosis in a histologically detailed computer model. *IEEE Transactions on Biomedical Engineering* 2013;**60**(8):2339–2349.
- [67] Ben-Haim SA, Osadchy D, Scnuster I, Gepstein L, Hayam G, Josephson ME. Nonfluoroscopic, in vivo navigation and mapping technology. *Nature Medicine* 1996;**2**(12):1393–1395.
- [68] Lloyd-Jones DM, Wang TJ, Leip EP, Larson MG, Levy D, Vasan RS, D'Agostino RB, Massaro JM, Beiser A, Wolf PA, Benjamin EJ. Lifetime risk for development of atrial fibrillation: the Framingham heart study. *Circulation* 2004;**110**(9):1042–1046.
- [69] Feuer EJ, Wun LM, Boring CC, Flanders WD, Timmel MJ, Tong T. The lifetime risk of developing breast cancer. *Journal National Cancer Institute* 1993;**85**(11): 892–897.

9. Figure Legends

Figure 1

Title: Pre-ablation segmentation results.

Legend: Enhancement segmentation results on testing baseline LGE CMR data-sets of two randomly selected long-standing persistent AF patients (top: patient 1, bottom: patient 2). Left: original data-

sets, middle: segmented left atrial walls, right: classification results. A=anterior, P=posterior, L=left, R=right.

Figure 2

Title: Post-ablation segmentation results.

Legend: Enhancement segmentation results on testing three months post-ablation LGE CMR data-sets of two randomly selected long-standing persistent AF patients (top: patient 1, bottom: patient 2). Left: original data-sets, middle: segmented left atrial walls, right: classification results. A=anterior, P=posterior, L=left, R=right.

Figure 3

Title: CMR versus invasive electro-physiology.

Legend: Juxtaposition of 3D postero-anterior (PA) views of the left atrial wall tissue classified as "pre-existent fibrosis" [left, in gray –obtained from a baseline LGE CMR scan and projected onto the segmented left atrial blood-pool (LABP), shown in pink] and the registered bipolar voltage map [right –measured with a NavX EAM system: Healthy left atrial wall tissue is showing in purple, while gray represents low voltage tissue]. CMR scar map compares well to the corresponding endocardial bipolar voltage map.

Figure 4

Title: The relative extent of native fibrosis.

Legend: The relative extent of native fibrosis as measured from the baseline LGE CMR data-sets of the long-standing persistent AF patients of this study. Fibrotic tissue extent is expressed as a percentage of the overall left atrial wall volume.

Figure 5

Title: 3D volume renderings of the ablation lesions.

Legend: 3D volume renderings of the classified enhancement (in blue –obtained from a three months post-ablation LGE CMR data-set) overlaid upon the segmented left atrial blood-pool (LABP). Enhancement distribution comprised encirclement of each ipsilateral pair of pulmonary veins at their antra, as well as a linear pattern at the mitral isthmus, as might be expected by the respective ablation techniques. RSPV = right superior pulmonary vein, RIPV = right inferior pulmonary vein, LSPV = left superior pulmonary vein, LIPV = left inferior pulmonary vein, LAA = left atrial appendage.

Figure 6

Title: Comparison with threshold levels proposed by other studies on pre-ablation data-sets.

Legend: Comparison of enhancement segmentation techniques on a base-line LGE CMR data-set of a long-standing persistent AF patient. The threshold levels proposed in other studies ($T_{PRE} = 3$ for study cited in [18], and $T_{PRE} = 4$ for study cited in [19]) led to gross underestimations of the enhancement. A=anterior, P=posterior, L=left, R=right.

Figure 7

Title: Comparison with threshold levels proposed by other studies on three months post-ablation data-sets.

Legend: Comparison of enhancement segmentation techniques on a three months post-ablation LGE CMR data-set of a long-standing persistent AF patient. The threshold level proposed in another study ($T_{POST} = 3$ for study cited in [18]) led to gross underestimation of the enhancement. A=anterior, P=posterior, L=left, R=right.

Figure 8

Title: Regional variation in the reference region statistics.

Legend: Regional variation in the reference region statistics. The borders of the reference region within the left atrial blood-pool (LABP) are drawn in yellow. By choosing a larger area, the standard deviation of the signal intensity distribution also increased.

10. Tables

Table 1

Title: Pre-ablation threshold levels selected by expert observers.

Legend: The normalized intensity levels that were selected by the expert observers to mark out the lower boundary of enhanced tissue in the training ($N=7$) pre-ablation LGE CMR data-sets. Possible threshold levels ranged from 1 to 6 in increments of $1/8$.

	Observer 1	Observer 2	Observer 3
Patient 1	1 1/4	1 1/4	1 1/4
Patient 2	1 1/8	1 1/4	1 1/8
Patient 3	1 1/4	1 1/4	1 1/4
Patient 4	1 1/4	1 1/4	1 3/8
Patient 5	1 1/4	1 1/4	1 1/4
Patient 6	1 1/4	1 3/8	1 3/8
Patient 7	1 1/4	1 1/4	1 1/4

Table 2

Title: 3 months post-ablation threshold levels selected by expert observers.

Legend: The normalized intensity levels that were selected by the expert observers to mark out the lower boundary of enhanced tissue in the training ($N=10$) three months post-ablation LGE CMR data-sets. Possible threshold levels ranged from 1 to 6 in increments of $1/8$.

	Observer 1	Observer 2	Observer 3
Patient 1	1 5/8	1 5/8	1 5/8
Patient 2	1 5/8	1 5/8	1 5/8
Patient 3	1 4/8	1 5/8	1 4/8
Patient 4	1 5/8	1 5/8	1 5/8
Patient 5	1 6/8	1 5/8	1 5/8
Patient 6	1 5/8	1 5/8	1 5/8
Patient 7	1 5/8	1 5/8	1 5/8
Patient 8	1 5/8	1 5/8	1 5/8
Patient 9	1 5/8	1 6/8	1 6/8
Patient 10	1 5/8	1 5/8	1 5/8

Table 3

Title: Group statistics of the relative extent of native fibrosis.

Legend: The mean and standard deviation of the relative extent of native fibrosis, summarizing the measurements from the baseline LGE CMR data-sets of the long-standing persistent AF patients of this study. Fibrotic tissue extent is expressed as a percentage of the overall left atrial wall volume.

	Mean	Standard Deviation

Relative extent of native fibrosis (%)	26.14	11.17
---	-------	-------

Figure 1

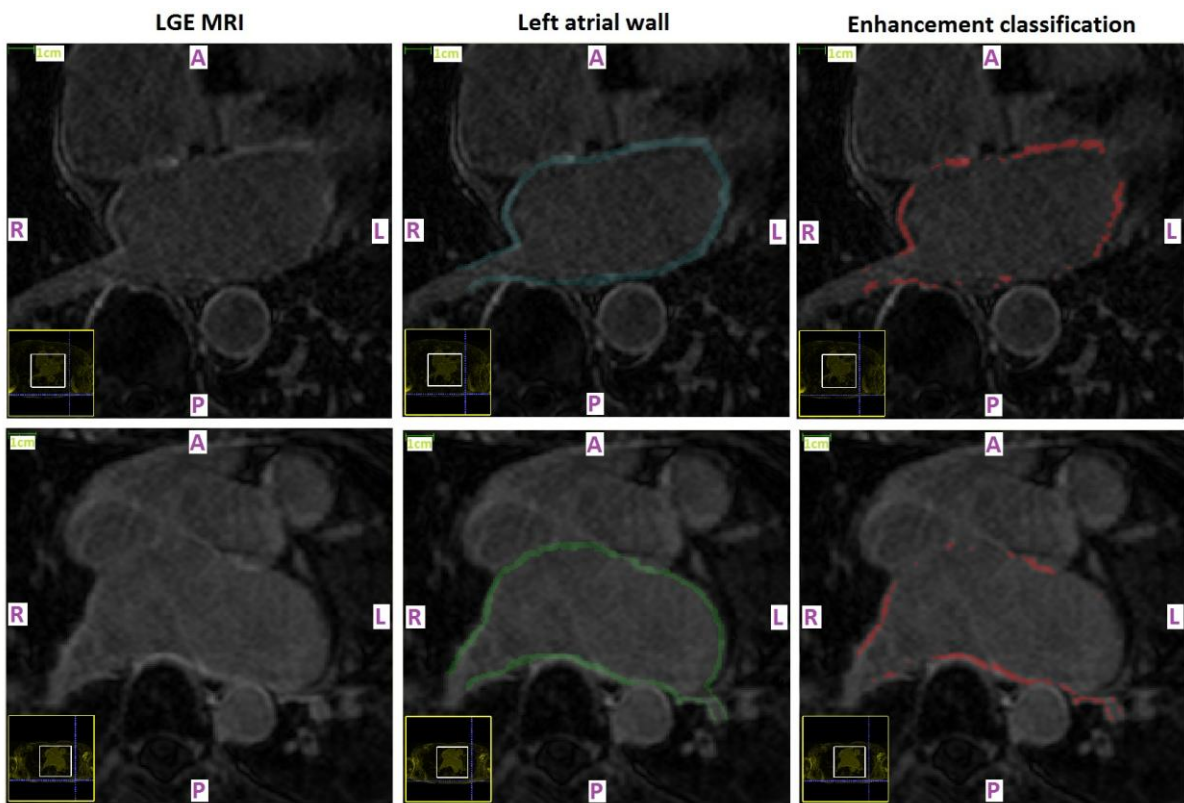


Figure 2

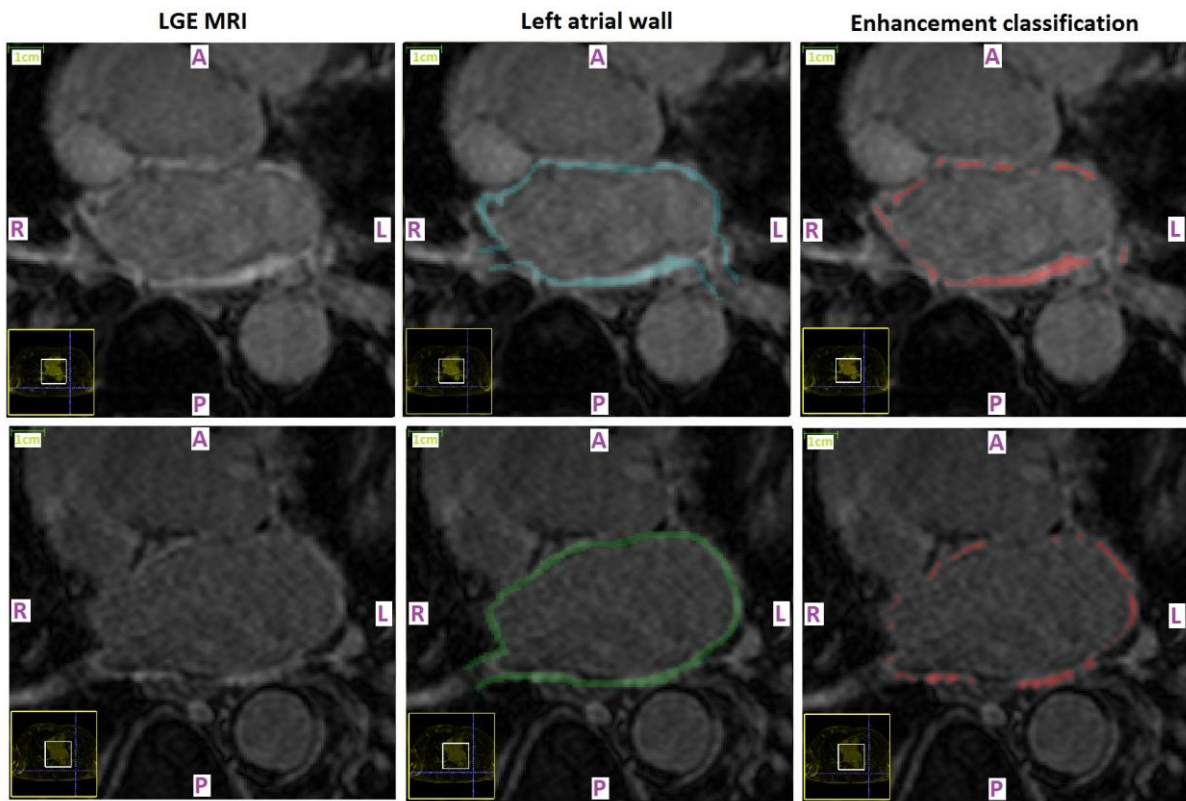


Figure 3

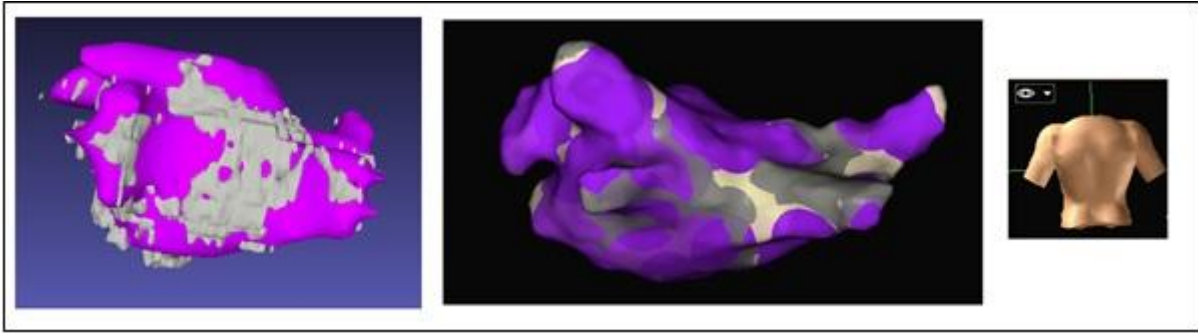


Figure 4

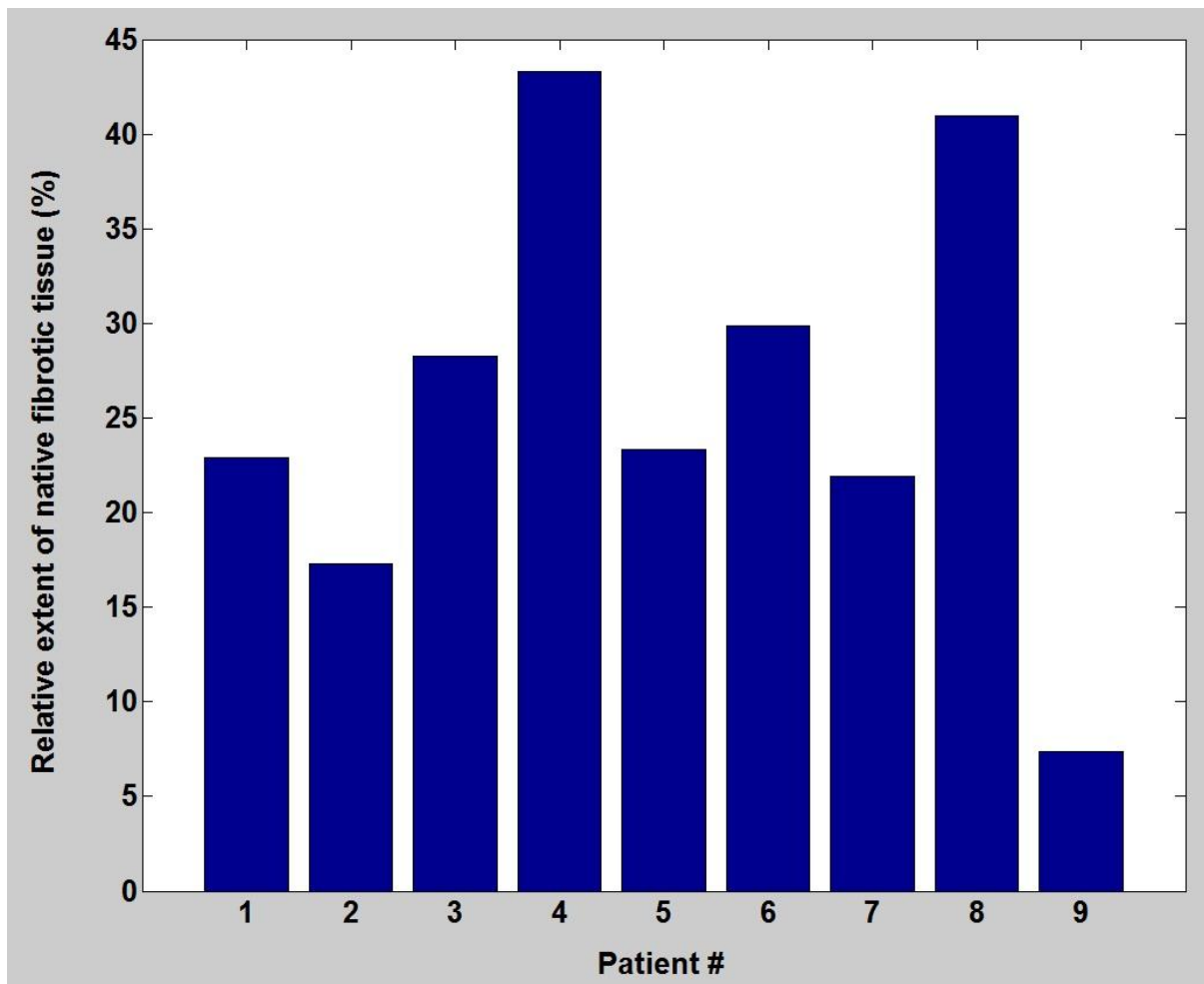


Figure 5

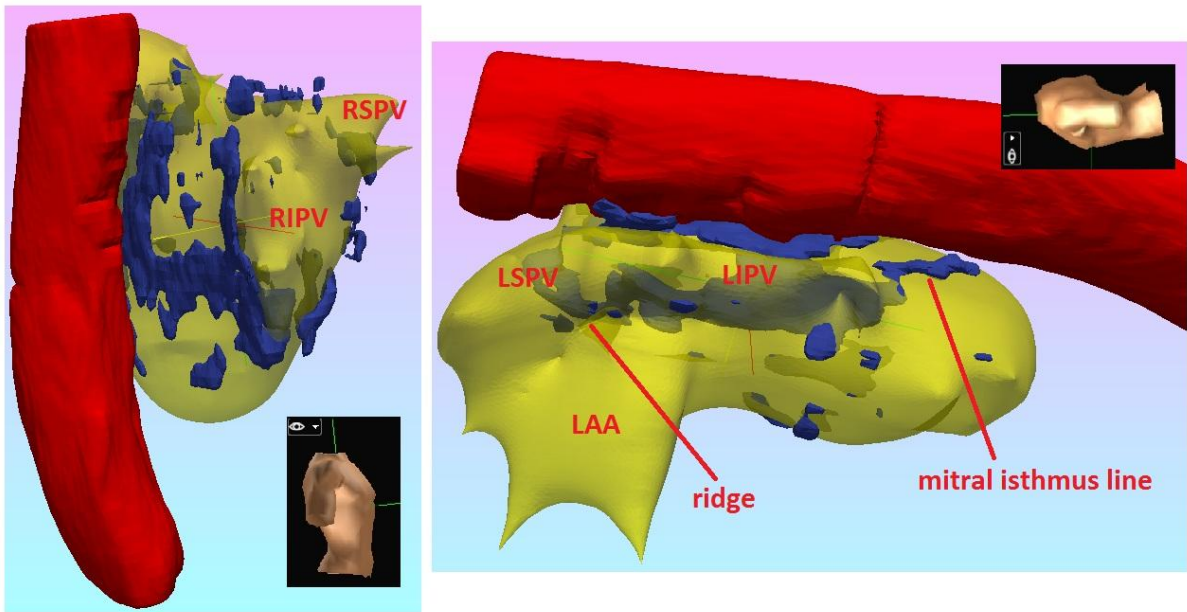


Figure 6

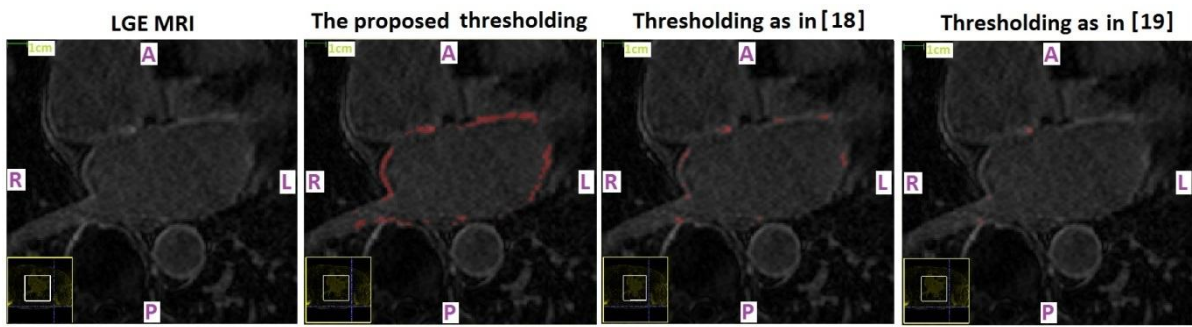


Figure 7

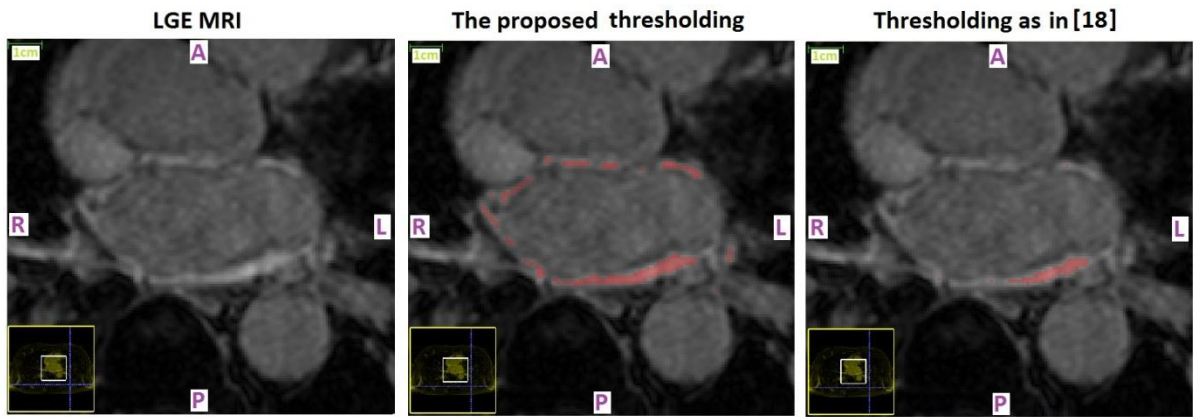
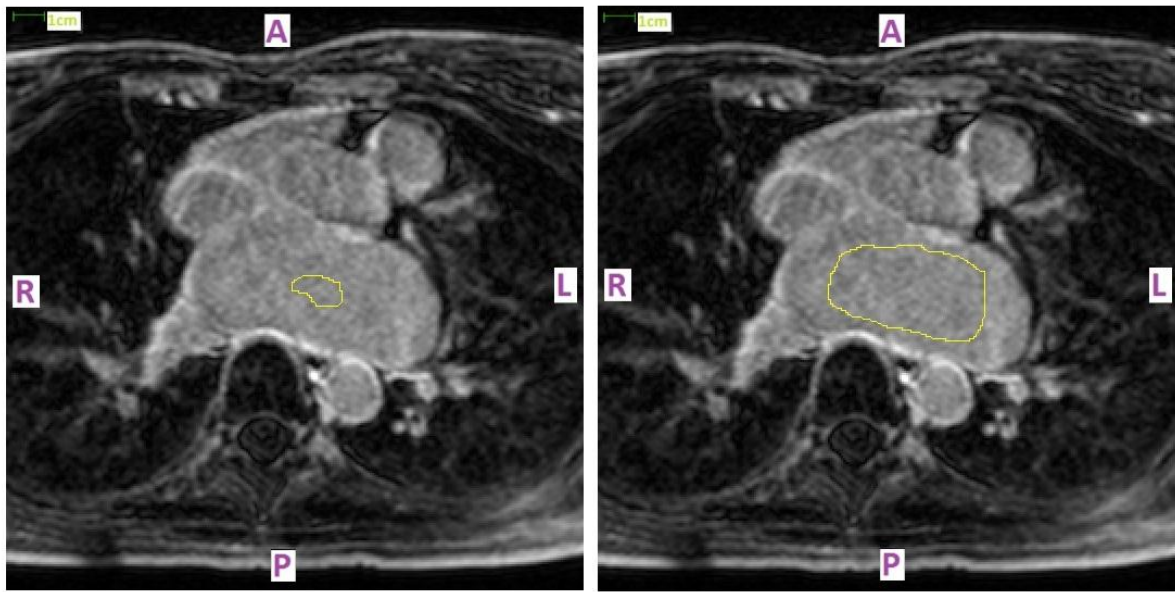


Figure 8



1

2

	Area	Mean	Std Dev	Min	Max
1	150.9	154.9	9.081	129	180
2	1427	156	12.101	122	211